

Radio Cosmology Lab

Exploring the Epoch of Reionization

Joshua Kerrigan, Adam Lanman, Wenyang Li, Jonathan Pober
Brown University Physics

Introduction

Following the recombination of hydrogen and release of the cosmic microwave background radiation, the baryonic matter of the universe consisted mostly of neutral hydrogen and helium. Gradually, small inhomogeneities collapsed and ignited into the first luminous structures. Energetic photons emitted from the first stars and quasars reionized the surrounding medium, producing ionized bubbles which grew and merged into the fully ionized intergalactic medium we see today. This *Epoch of Reionization* (EoR) remains a poorly-understood period of the universe's history which offers a wealth of cosmological and astrophysical information.

The Pober lab is part of an international effort to build instruments capable of studying the EoR. The neutral hydrogen (HI) of the EoR emits faintly at a wavelength of 21cm due to the hyperfine transition. This emission is unique to neutral hydrogen, and is anti-correlated with the ionized (HII) regions that fill the universe through the EoR. CMB constraints and quasar absorption spectra place the EoR within the redshift range $6 < z < 12$, which means 21cm emissions will reach us at meter scale wavelengths. This is accessible to modern radio interferometers, including the *Donald C. Backer Precision Array for Probing the Epoch of Reionization* (PAPER), the *Murchison Widefield Array* (MWA), and the recently-funded *Hydrogen Epoch of Reionization Array* (HERA). Extracting this weak signal remains a challenge unprecedented in radio astronomy.

Differential Brightness Temperature

$$\delta T_b = 27(1 + \delta) x_{\text{HI}} \left(1 - \frac{T_{\text{CMB}}}{T_{\text{spin}}} \right) \left(\frac{\Omega_b h^2}{0.0223} \right) \left(\frac{1 + z}{10} \frac{0.15}{\Omega_m h^2} \right)^{1/2} \left[\frac{H(z)/(1+z)}{\partial_r v_r} \right] \text{ mK}$$

Density perturbation Neutral fraction Spin excitation Baryon and matter mass fractions Peculiar velocities

The differential brightness temperature δT_b is the contrast between the intensity of 21 cm emissions/absorptions against the Cosmic Microwave Background. Its full expression is related to cosmological (green) and astrophysical (red) parameters. Figure 1 shows the evolution of the spherically-averaged *global* 21 cm brightness temperature.

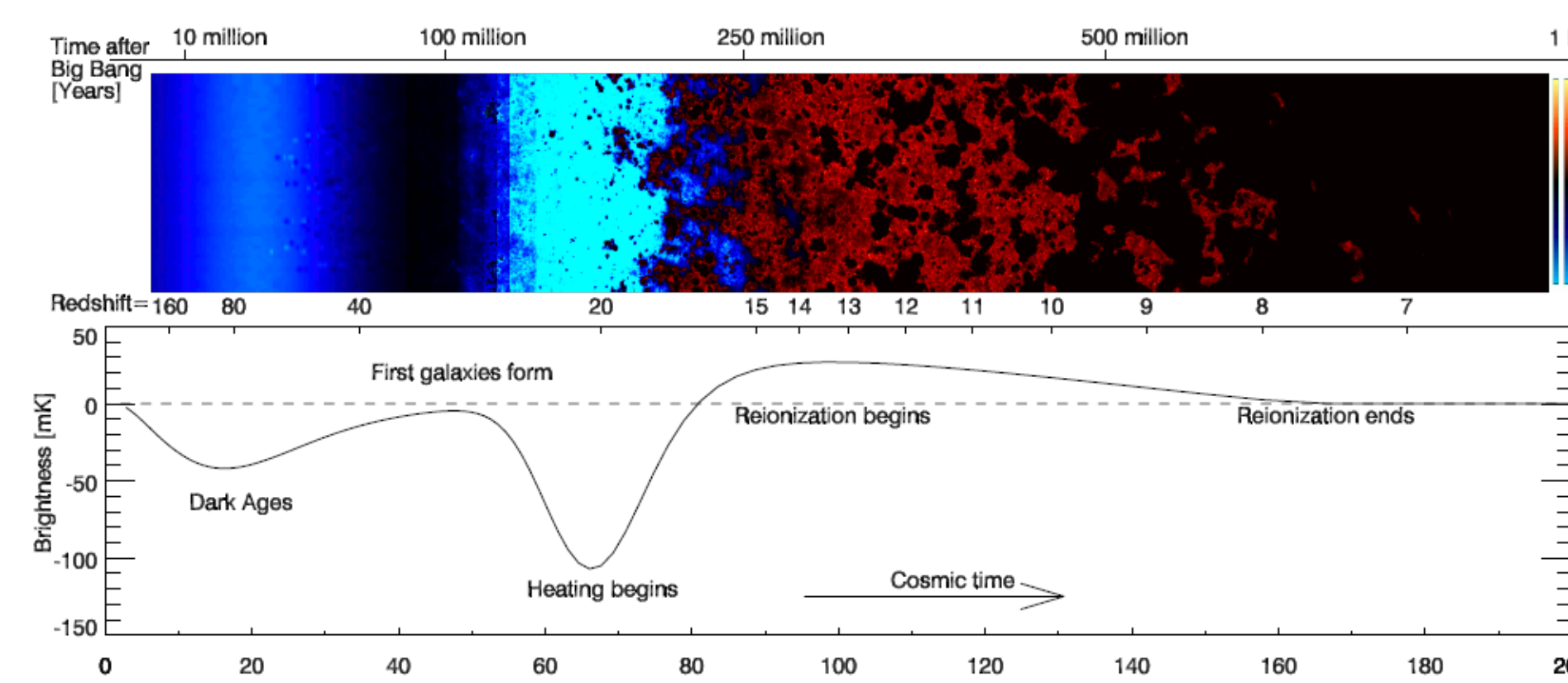


Figure 1: The global differential brightness temperature, δT_b , evolution over redshift $6 < z < 160$. δT_b becomes observable when the spin temperature T_s decouples from the CMB temperature, T_{CMB} . Eqn. ???. Source: Pritchard & Loeb. Nature 468.7325 (2010): 772-773.

The Foreground Problem

The expected EoR signal is ~ 5 orders of magnitude smaller than known foreground sources, such as diffuse emission from the Galaxy and extragalactic point sources. Removing these foregrounds, as well as instrumental noise, is a nontrivial problem. The overlapping sources of power in our observations can be seen in Fig. 2.

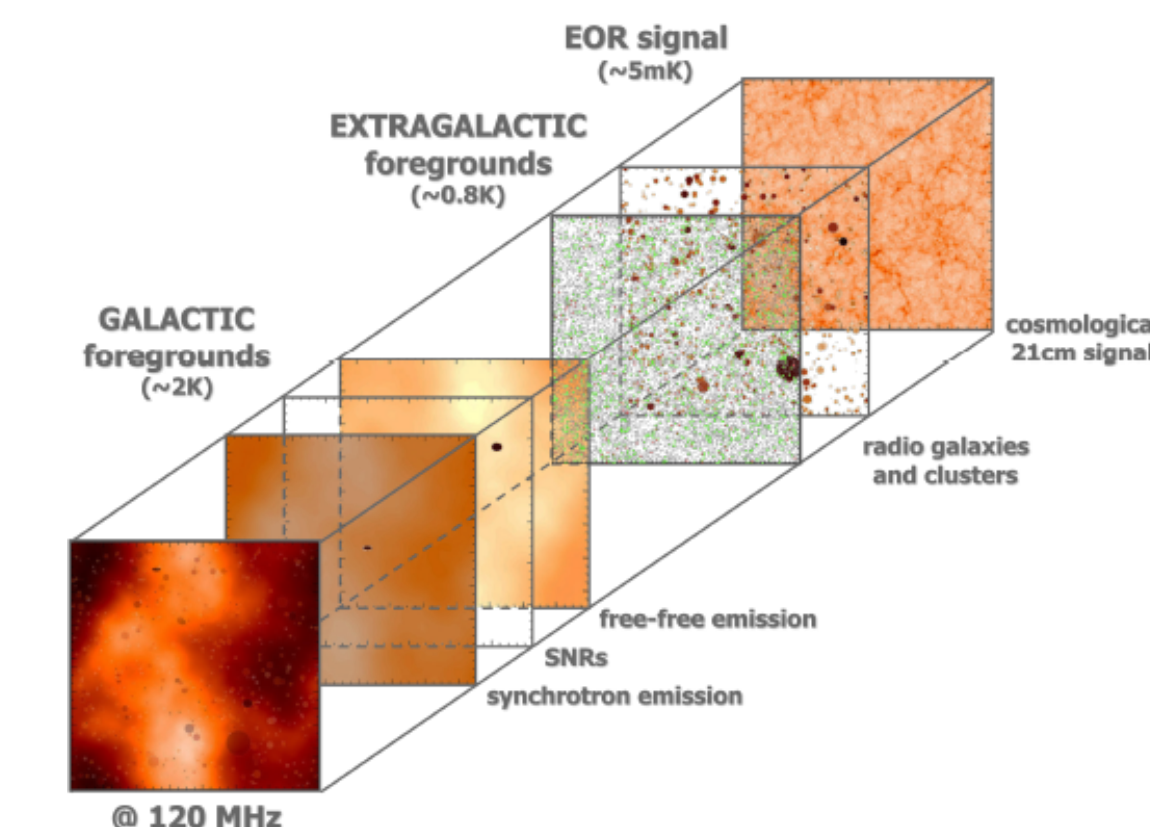


Figure 2: The various cosmological and galactic sources that contribute to the measured sky temperature, and their relative strengths.
Source: Zaroubi, Saleem. 'The First Galaxies'. Springer Berlin Heidelberg, 2013. 45-101.

To overcome foreground dominance in our power spectrum analysis we can use a combination of foreground power mitigating techniques as outlined in the following subsections.

Foreground Subtraction

Foreground subtraction is performed in the image domain using an extragalactic source catalog. The source catalog is used to generate a foreground model which can then be fit by an n^{th} order polynomial and subtracted from the observation.

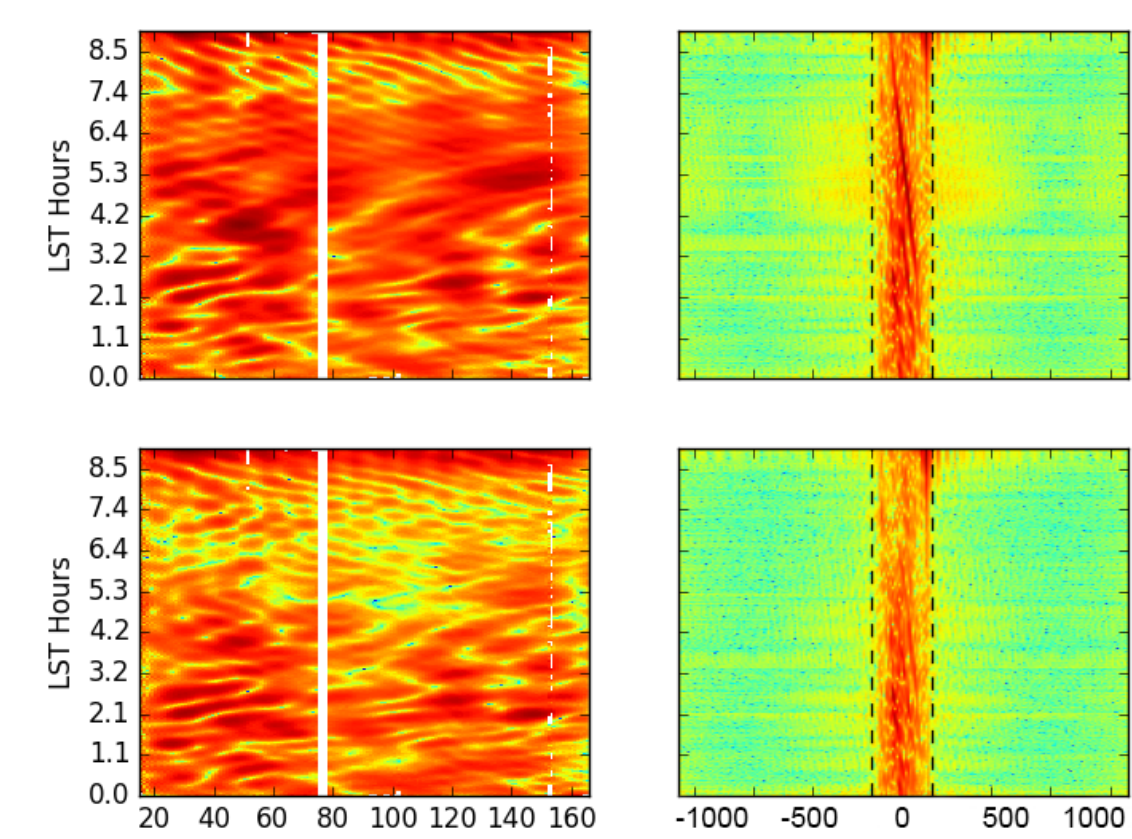


Figure 3: LST binned visibility of a 30m East-West baseline from the PAPER-64 array. The left plots show a baseline visibility pre- and post subtraction. The right plots show the delay transform of the left plots, demonstrating the foreground power being concentrated within the horizon limit (dotted lines).

Foreground Avoidance

$$V_b(\tau) = \int d\ell dm dv \mathcal{A}(\ell, m, v) I(\ell, m, v) e^{-2\pi i v(\tau_g - \tau)} \quad (1)$$

Equation 1 demonstrates the *delay transform*: A Fourier transform of frequency to its conjugate *delay*. There is a natural limit in delay, set by the time it takes light from a source at the horizon to travel between the two antennas of a baseline. Power from foreground sources is confined within this *horizon limit*, as shown by Figs. 3 & ??.

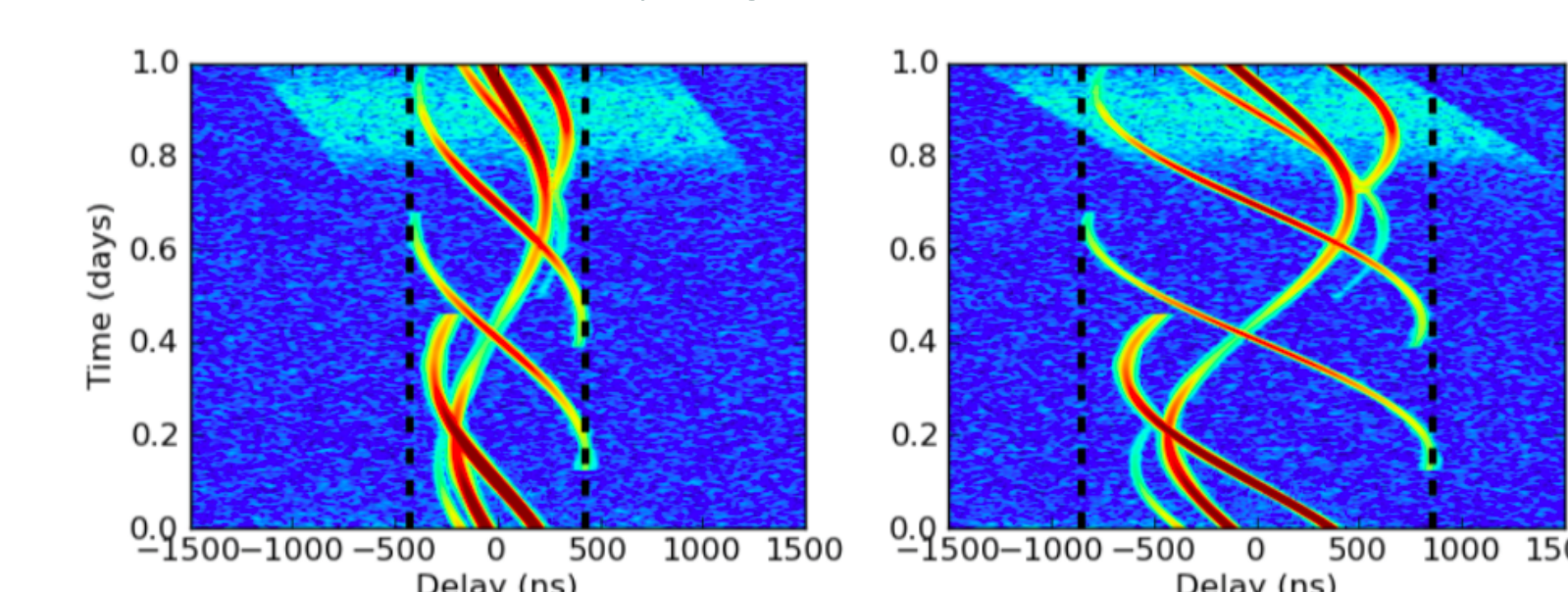
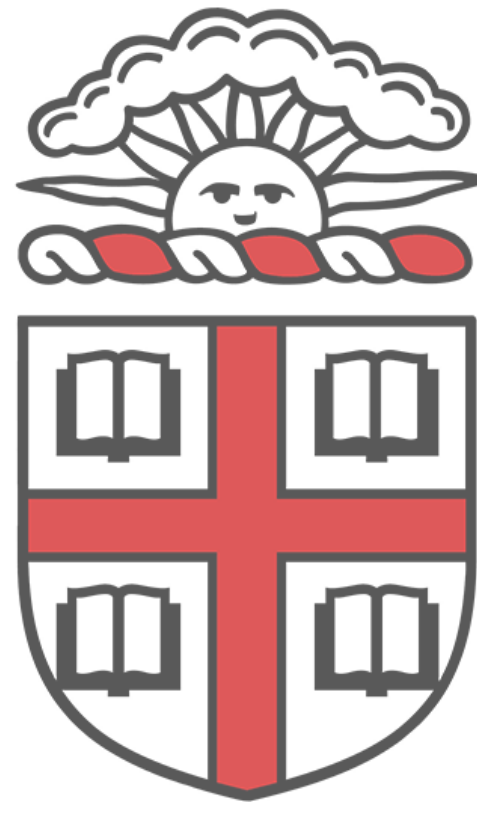


Figure 4: Delay transform visibilities of two different baseline types. Smooth spectral sources moving between delays over time can be seen to remain within the horizon limit (dotted), while unsmooth spectral sources (light blue) extend beyond the horizon limit.
Source: Aaron Parsons, *A Per Baseline Delay-Spectrum Technique for Accessing the 21cm Cosmic Reionization Signature*, ApJ. 2012

21 cm COSMOLOGY @



Radio Telescope Arrays



Figure 7: PAPER - A first-generation array located in the Karoo desert of South Africa. Designed specifically for EoR research, PAPER is designed for maximum redundancy. Several baselines sample each k_{\perp} modes, which allows for the use of redundant calibration.



Figure 8: MWA - Located in Western Australia at the Murchison Radio Astronomy Observatory. The MWA serves multiple functions, including ionosphere studies and detection of transient radio signals. Phase I consisted of 128 tiles which are each made up of 16 dipole antennae. The Phase I configuration maximized uv coverage, improving imaging capability. It has since been partially reconfigured into Phase II, which includes two hexagonal grids of tiles designed for high-redundancy EoR research. MWA is a pathfinder project for the Square Kilometer Array (SKA).



Figure 9: HERA - Located at the same site as PAPER in the Karoo desert. The current phase of HERA consists of 19 14m parabolic dishes. In its final form, HERA will comprise 331 dishes in a closely-packed hexagonal grid. HERA is also a pathfinder project for the SKA.

Simulation

The particular characteristics of an array can introduce unexpected effects into the data. Understanding and mitigating instrumental effects is critical to making a confident detection of the EoR. For this reason, much effort has been put into simulating the full analysis pipeline – from the point and diffuse sources on the sky, to the raw visibilities that come out of the correlator, to the power spectrum estimations.

Fast Holographic Deconvolution (FHD) is a purpose-built software framework for analyzing MWA data. FHD does foreground subtraction by *forward modeling*, which builds a simulated data set, including instrumental effects, and subtracts it from the actual data. This forward modeling feature can also be used as a standalone simulation tool, to generate raw visibilities of foregrounds, noise, and EoR off of existing and future 21cm experiments.

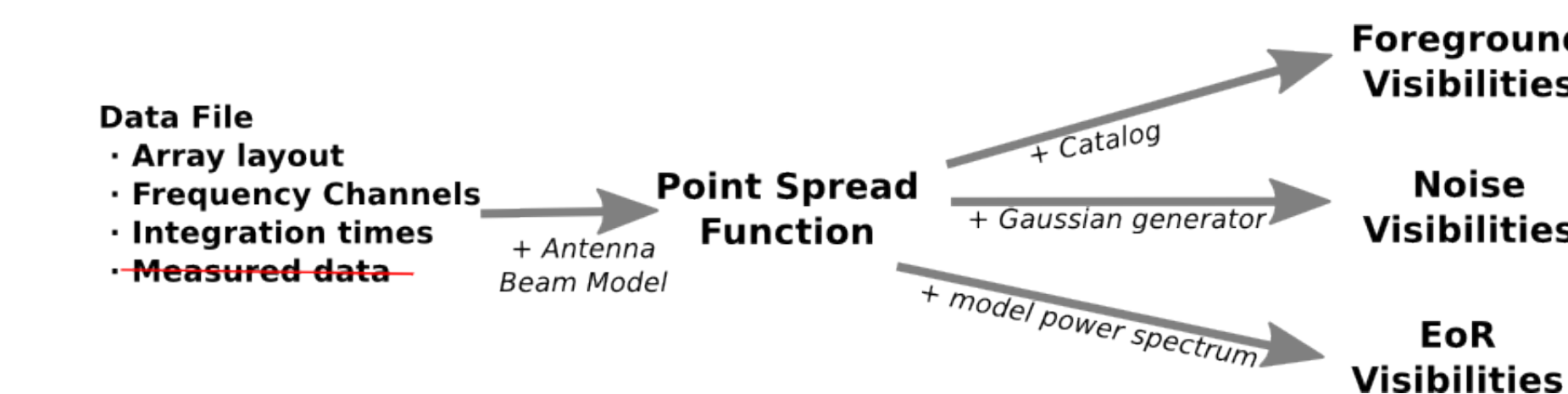


Figure 5: A sample data file (or generated data file) holds array coordinates over time and the frequency channels of the instrument. Given a beam model for the antenna, FHD calculates the full synthesized beam (or point-spread function) for a particular time and set of frequencies. The synthesized beam can then convert a sky catalog into a set of foreground visibilities for the instrument. External EoR simulations can also be fed in to test EoR sensitivity, or Gaussian noise can be injected to simulate noise.

Calibration

21 cm observations of the Epoch of Reionization (EoR) have the potential to reveal a wealth of information about the formation of the first stars and galaxies by measuring the three dimensional power spectrum and full tomographic maps of the neutral IGM. However, these observations are technically very challenging due to bright astrophysical foregrounds and the chromatic nature of radio interferometers. In the last two years it has become apparent that precision instrument calibration is crucial for disentangling the faint cosmological signal from the bright foregrounds. Current precision calibration efforts for EoR observations fall into two camps: sky based calibration using deep foreground catalogs and forward modelling of the instrument visibilities, and redundant calibration that foregoes a sky model but requires the tiles be placed on a precise grid.

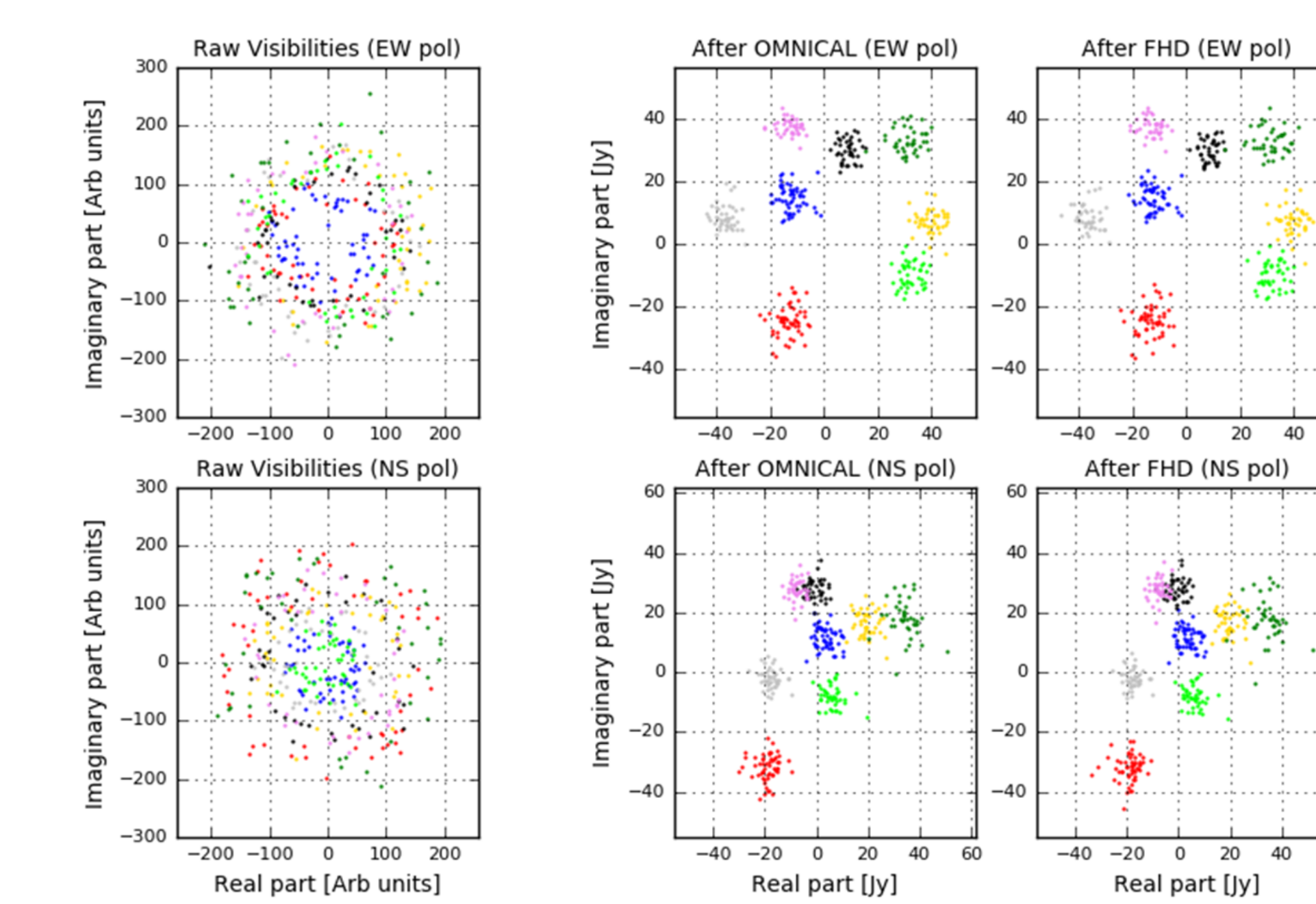


Figure 6: 2 min averaged complex visibilities of EoR observation by MWA II at 191MHz from 8 redundant baseline groups. Each color represents one baseline group. Left column: raw visibilities, with arbitrary units; Middle column: visibilities after OMNICAL, with degeneracy parameters projected (units: Jy); Right column: visibilities after FHD sky calibration (units: Jy). Top row: East-West polarization; Bottom row: North-South polarization.